Available online at www.sciencedirect.com
ScienceDirect
Journal of Power Sources 172 (2007) 713–724
JOURNAL OF POWER SOURCES
www.elsevier.com/locate/jpowsour

A model for solid oxide fuel cell (SOFC) stack degradation

Anil V. Virkar

Department of Materials Science & Engineering, University of Utah, Salt Lake City, UT 84112, USA

Received 9 May 2007; accepted 17 May 2007
Available online 25 May 2007

Abstract

Solid electrolytes are increasingly being used in active electrochemical devices such as fuel cells and batteries. Several fuel cells or batteries are connected in series to form a stack or a battery pack. The present manuscript examines the phenomenon of degradation in such devices, whose origin lies in the very basics of local thermodynamic equilibrium and transport. The specific example of solid oxide fuel cells (SOFC) is addressed here. If a single cell (or a few cells) in a stack exhibits higher resistance than the rest of the cells, stack failure often initiates at such a cell. The cell is then driven by, and exhibits lower voltage than the rest of the cells, and often even a negative voltage. The objective of this paper is to present a model for stack degradation when one of the cells exhibits a negative voltage. The existence of low level electronic conduction through the electrolyte plays central role in degradation. It is shown that if a cell exhibits a negative voltage, the oxygen chemical potential within the electrolyte can exceed that in the oxidant, and/or can drop below that in the fuel. This can lead to high internal oxygen partial pressure resulting in electrode cracking and delamination, and/or very low oxygen partial pressure leading to local electrolyte decomposition. Both situations can lead to cell and stack degradation.

Keywords: Solid oxide fuel cell; Stack; Degradation

1. Introduction

Over the past four decades, the interest in active electrochemical devices based on solid electrolytes has steadily grown. By active is meant a device through which substantial amount of current is passed during its operation, in contrast to devices such as potentiometric sensors. The interest in solid electrolytes is due to their potential advantages over liquid electrolytes, namely: (a) wider temperature range of operation; and (b) electrolyte management is not an issue as the electrolyte is solid. Examples of prominent solid electrolytes currently being pursued in active electrochemical devices include sodium beta" alumina ($Na_2O{\cdot}\sim 6Al_2O_3$)—a sodium ion conductor, for applications in sodium–sulfur batteries, sodium–metal salt batteries, electrochemical thermoelectric generators; and yttria-stabilized zirconia (YSZ) for SOFC, electrolyzers, and electrochemical oxygen separation from air. Many of the solid electrolytes, such as sodium beta" alumina, have been often referred to as super ionic conductors since their ionic conductivity compares well with liquid electrolytes such as molten salts. It is this feature which has attracted considerable attention over the past several decades. Even though there exist solid electrolytes with very high ionic conductivities, they differ from liquid electrolytes (e.g. aqueous solutions of salts and molten salts) in two very important aspects. In liquid electrolytes, both cations and anions exhibit high mobilities/diffusivities. Thus, they both can respond and adjust to external/internal stimuli. Also, being liquid, any local volume changes that may occur during transport can be easily accommodated. In solid electrolytes, however, usually only one type of an ion (either a cation or an anion) exhibits high mobility/diffusivity. As a consequence, electronic species (electrons and/or holes) play a key role in the establishment of local equilibrium. Also, being a solid, any changes that may occur in volume cannot be easily accommodated, and can result in locally high stresses causing cracking or delamination. While the approach presented in this manuscript and the resulting conclusions should be applicable to a host of devices based on solid electrolytes, the discussion presented here is mainly confined to solid oxide fuel cells (SOFC).

A typical SOFC consists of three components: (a) a porous cathode; (b) a porous anode; (c) a dense, ceramic ionic conductor (usually an oxygen ion, O^{2-}, conductor) sandwiched between the cathode and the anode. The porous cathode is

E-mail address: anil.virkar@m.cc.utah.edu.

0378-7753/$ – see front matter © 2007 Elsevier B.V. All rights reserved.
doi:10.1016/j.jpowsour.2007.05.076

Nomenclature

e	electronic charge (C)
E	open circuit voltage (V)
E_0	Nernst voltage (V)
E^{a}	internal EMF across anode/electrolyte interface in the equivalent circuit (V)
E^{c}	internal EMF across cathode/electrolyte interface in the equivalent circuit (V)
E^{el}	internal EMF across electrolyte (just inside interfaces) in the equivalent circuit (V)
F	Faraday constant (C mol^{-1})
I	measured current density (A cm^{-2})
I_{i}	ionic current density through the membrane (A cm^{-2})
I_{e}	electronic current density through the membrane (A cm^{-2})
k_{B}	Boltzmann constant (J $^{\circ -1}$)
ℓ	membrane thickness (cm)
$p_{\mathrm{O_2}}$	oxygen partial pressure (atm)
$r_{\mathrm{e}}^{\mathrm{a}}$	anode area specific electronic charge transfer resistance (Ω cm^2)
$r_{\mathrm{e}}^{\mathrm{c}}$	cathode area specific electronic charge transfer resistance (Ω cm^2)
$r_{\mathrm{i}}^{\mathrm{a}}$	anode area specific ionic charge transfer resistance (Ω cm^2)
$r_{\mathrm{i}}^{\mathrm{c}}$	cathode area specific ionic charge transfer resistance (Ω cm^2)
$r_{\mathrm{e}}^{\mathrm{el}} = \rho_{\mathrm{e}}^{\mathrm{el}}\ell$	electrolyte area specific electronic resistance (Ω cm^2)
$r_{\mathrm{i}}^{\mathrm{el}} = \rho i_{\mathrm{e}}^{\mathrm{el}}\ell$	electrolyte area specific ionic resistance (Ω cm^2)
R	ideal gas constant (J ($^{\circ}$ mol)$^{-1}$)
R_{C}	area specific resistance of the cell with high resistance ('bad' cell) (Ω cm^2)
R_{L}	load (Ω cm^2)
R_{N}	area specific resistance of a cell exhibiting normal behavior (Ω cm^2)
$R_{\mathrm{i}} = r_{\mathrm{i}}^{\mathrm{c}} + r_{\mathrm{i}}^{\mathrm{el}} + r_{\mathrm{i}}^{\mathrm{a}}$	cell area specific ionic resistance (Ω cm^2)
$R_{\mathrm{e}} = r_{\mathrm{e}}^{\mathrm{c}} + r_{\mathrm{e}}^{\mathrm{el}} + r_{\mathrm{e}}^{\mathrm{a}}$	cell area specific electronic resistance (Ω cm^2)
v_{c}	volume of pore or a void in the electrolyte at the cathode/electrolyte interface (cm^3)
V_{C}	cell voltage (V)

Greek symbols

δ	interfacial thickness (cm)
η_{act}	activation polarization (V)
λ	a geometric parameter describing the pore or void (cm^2)
μ_i	chemical potential of species i (J mol^{-1} or J species^{-1})
$\tilde{\mu}_i$	electrochemical potential of species i (J mol^{-1} or J species^{-1})
$\rho_{\mathrm{e}}^{\mathrm{el}}$	electronic resistivity of the membrane (Ω cm)
$\rho_{\mathrm{i}}^{\mathrm{el}}$	ionic resistivity of the membrane (Ω cm)

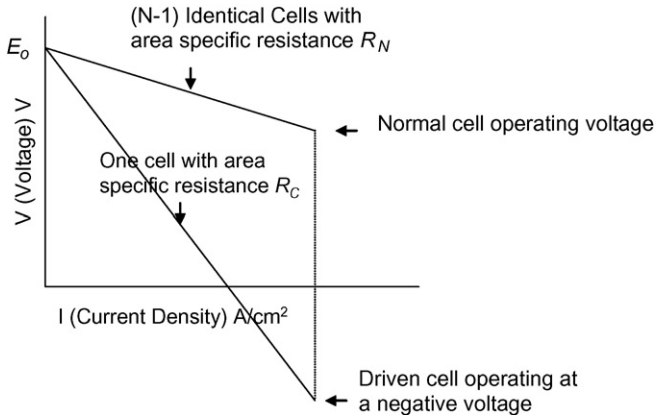

Fig. 1. Voltage/cell vs. current density plots for a stack with one cell exhibiting much greater resistance than the rest of the cells, and exhibiting a negative voltage under operating conditions.

usually a composite of an electronic (ceramic) conductor and an oxygen ion conductor. The porous anode consists of a mixture of a metal, such as nickel, and an oxygen ion conductor. At the cathode, reduction of oxygen molecules, O_2, to oxygen ions, O^{2-} occurs. The oxygen ions, O^{2-}, transport through the electrolyte towards the anode. At the anode, O^{2-} reacts with gaseous fuel, H_2 or $H_2 + CO$, to form H_2O or $H_2O + CO_2$, and release electrons which transport in the external circuit to the cathode.

A typical planar solid oxide fuel cell (SOFC) stack comprises a number of cells connected in series with each repeat unit consisting of a cell, interconnect separator and flow channels on either side of the cell. Results on stacks containing upwards of one hundred cells in series have been reported. Connecting a large number of cells in series is necessary in order to build up the voltage to some useful value and also for realizing significant amount of power generating capacity in a compact space. It is necessary that cell-to-cell (or repeat unit to repeat unit) characteristics be as uniform as possible including contact between repeat units. If this is achieved, it ensures that at a given operating current, the voltage across each cell (or repeat unit) is essentially the same. If, however, not all cells/repeat units are identical, the voltages across the individual cells/repeat units will be different. Differences in voltages are directly related to differences in cell/repeat unit resistances. In many instances, it has been noted that even if the initial voltages are essentially uniform indicating little difference in cell-to-cell resistance, over time one or more cells exhibit different behavior—namely a different voltage at a given current indicating a different resistance. A common observation is that over time the resistance of one or more cells increases in relation to the rest of the cells leading to a greater voltage drop across such a cell (or lower operating cell voltage, V_C) or cells at a given current than the rest of the cells. In such a case, it is often stated that the rest of the cells (the rest of the stack) drive(s) the cell with higher resistance. In the extreme case, the voltage across such a cell may become negative under operating conditions. That is, across such a cell (repeat unit), the voltage $V_C = E - IR_C < 0$, where E is the open circuit voltage, I is the current density, and R_C is the area specific resistance of that cell or repeat unit. Fig. 1 shows a schematic representa-

tion of such a situation. It has been observed that when such a deviation from the normal behavior sets in, it eventually leads to cell failure, which reflects as a loss of voltage, and increase in local temperature. This phenomenon then spreads to adjacent cells almost as a domino effect. Postmortem often shows re-oxidation of the anode especially in anode-supported cells, and in some cases anode undergoes total destruction. So severe can be the destruction that one is left to speculate the cause (or causes) primarily based on postmortem observations and often without a clear theoretical basis. Also, interpretation based on postmortem alone may be misleading. For example, it is often stated that under high current densities, the partial pressure of water vapor formed (and effectively oxygen partial pressure) at the anode/electrolyte interface may be high enough to oxidize nickel in the anode. As will be discussed in this manuscript, such an interpretation could be erroneous, and the observed destruction of the anode may have occurred well after critical damage to the cell had already set in. That is, the observed re-oxidation of the anode may simply be a manifestation of the 'end of life' situation—and not the root cause.

There are many likely reasons why an isolated cell (or few cells) may develop a high resistance during operation. These include the formation of local hot spots leading to local changes in microstructures and in materials properties, small initial compositional in-homogeneities resulting in greater changes in properties, contact aid and/or electrode delaminations due to thermal cycling/rapid heating, reaction between electrode and electrolyte forming a high resistance layer, fuel and/or oxidant mal distributions, non-uniform oxidation of the interconnect, degradation of the seals, etc. It can be envisaged that there may be multitude of reasons why some cells may become 'bad' over a period of time. It is not objective of this manuscript is to scrutinize the various possible reasons why some cells develop high resistance. The objective of this manuscript is to provide a plausible mechanism for the occurrence of subsequent cell (and stack) degradation, once deviation (one or few cells exhibiting considerably greater resistance than the rest of the cells) sets in.

Typical SOFCs are based on an oxygen ion, O^{2-}, conducting solid electrolyte such as yttria-stabilized zirconia (YSZ), which is predominantly an oxygen ion conductor, with negligible conductivity for electronic (electron or hole) transport. Nevertheless, description of transport through YSZ (and other oxygen ion conductors as well as mixed-ionic electronic conductors, MIEC) is based on the assumption of local equilibrium. That is, virtually all transport problems reported in the literature are based on an explicit or implicit assumption of local (thermodynamic) equilibrium [1,2]. Even so, often the implications of local equilibrium are ignored in the analysis of transport. The local equilibrium of interest in predominantly oxygen ion conducting materials is given by

$$\tfrac{1}{2}O_2(\vec{r}) + 2e'(\vec{r}) \Leftrightarrow O^{2-}(\vec{r}) \quad (1)$$

where $\vec{r}$ is any position in the system. This assumption of local equilibrium (which is actually a requirement for conducting any kind of an analysis [1]) implies:

$$\tfrac{1}{2}\mu_{O_2}(\vec{r}) + 2\mu_e(\vec{r}) = \mu_{O^{2-}}(\vec{r}) \quad (2)$$

and

$$\tfrac{1}{2}\mu_{O_2}(\vec{r}) + 2\tilde{\mu}_e(\vec{r}) = \tilde{\mu}_{O^{2-}}(\vec{r}) \quad (3)$$

where μ's denote chemical potentials and $\tilde{\mu}$'s denote electrochemical potentials. The above implies that the existence of chemical potential of oxygen as a gas in a fully dense solid is perfectly appropriate and at local equilibrium equation (3) provides its relationship to electrochemical potentials of O^{2-} and e' [6]. The assumption of local equilibrium has very important implications, the most important one being that even in a predominantly ionic conductor, the electronic current cannot be entirely neglected [6]. That is, even though the magnitude of the electronic current in a typical ionic conductor is often negligible in comparison to the ionic current, it still cannot be set identically to zero. This is because the electronic transport, however small, plays a decisive role in the establishment of the above equilibrium and thus in the establishment of the local chemical potential of oxygen, $\mu_{O_2}(\vec{r})$, which in turn dictates the very stability of the membrane [3–7].

It is well recognized that properties in solids in the near surface regions are in general different than in the bulk. In ionic solids, for example, there often exists a region of space charge near free surfaces. Regardless of the presence of space charge, which can extend over large distances, the near surface regions are always expected to exhibit different properties than the bulk region. This is because the bond lengths of surface atoms, due to the presence of unsatisfied bonds, are slightly different than the interior bond lengths. The region of slightly different bond lengths, for example, may exist over only a few angstroms, but is not of zero thickness. Indeed, a computational study on silicon (Si(0 0 1)) has shown that such a layer, the origin of which lies in the presence of unsatisfied bonds on the surface, a characteristic of all condensed materials, extends about three to five atomic layers [8]. Such a region near the surface can be appropriately referred to as the interfacial region wherein the 'interface' has some finite thickness, which could be a few angstroms or nanometers. Fig. 2 shows a schematic representation of a membrane in contact with a gas (or could also be a liquid), wherein the thickness of this interfacial region, δ, is much smaller than the membrane thickness, ℓ. It is through this region of the solid that transport of *both* ions and electrons must occur, and only outside this region (at the gas phase/solid boundary) would it be reasonable to write the reaction:

$$\tfrac{1}{2}O_2(\text{gas}) + 2e'(\text{electrode}) \rightarrow O^{2-}(\text{solid electrolyte}) \quad (4)$$

Once again, the electronic current through the membrane (and thus also across the 'interfaces') may be very small, but is not mathematically zero. This is a significant departure from the usual description of electrode processes in solid-state electrochemical devices based on predominantly ionic conducting materials, in which only the ionic transport is assumed to occur through the membrane and electron participation is exclusively attributed to the overall charge transfer reaction given by Eq. (4).

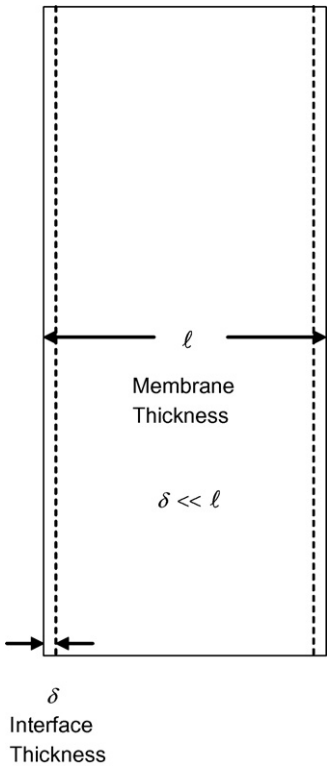

Fig. 2. A schematic representation of a solid electrolyte membrane of thickness ℓ in contact with a gas phase. The interfacial thickness is δ, which in general could be different at the two surfaces. The existence of the 'interfacial' region or the interface is related to different bond lengths of surface atoms/ions as compared to bulk atom/ions due to unsatisfied bonds on the surface. Such an interfacial region may only be a few atomic layers thick. This interfacial region is in addition to other surface layers, such as space charge layers, the latter extending over much greater distances. In the schematic, the interface thickness is shown exaggerated in comparison to the membrane thickness, ℓ.

The occurrence of transport of both ions and electrons across interfaces has important implications concerning the spatial variation of chemical potentials. Consider a membrane exposed to two different chemical potentials of oxygen in the gas phase; $\mu^{\mathrm{I}}_{\mathrm{O}_2}$ at one surface (electrode I) and $\mu^{\mathrm{II}}_{\mathrm{O}_2}$ at the other surface (electrode II) such that $\mu^{\mathrm{I}}_{\mathrm{O}_2} \neq \mu^{\mathrm{II}}_{\mathrm{O}_2}$. Assuming interface thicknesses to be much smaller than the membrane thickness but still nonzero, that is $0 < \delta \ll \ell$, it can be shown that there will always be abrupt (sharp) changes in μ_{O_2} across the two gas–solid interfaces; that is $\Delta\mu^{\mathrm{interface}}_{\mathrm{O}_2} \neq 0$ [6]. Thus, when determining an average of any μ_{O_2}-dependent property of the membrane (with $\mu^{\mathrm{I}}_{\mathrm{O}_2} \neq \mu^{\mathrm{II}}_{\mathrm{O}_2}$), such as for example ambipolar conductivity, the integration limits cannot be taken as $\mu^{\mathrm{I}}_{\mathrm{O}_2}$ and $\mu^{\mathrm{II}}_{\mathrm{O}_2}$ even if the electrodes are reversible [6,7]. This implies that the commonly made assumption of the equilibration of chemical potential of oxygen, μ_{O_2}, in the gas phase with the adjacent region of the solid is not accurate in all cases of interest where $\mu^{\mathrm{I}}_{\mathrm{O}_2} \neq \mu^{\mathrm{II}}_{\mathrm{O}_2}$ [9].

Denoting ionic current density by I_{i} and electronic current density by I_{e}, the above implies that, even in a predominantly ionic conductor such as YSZ with $|I_{\mathrm{i}}| \gg |I_{\mathrm{e}}|$, it is understood that $I_{\mathrm{e}} \neq 0$. Analysis conducted recently leads to the following general conclusions [6,7].

1.1. Directions of ionic and electronic currents and chemical potential of oxygen in the membrane

If the directions of ionic current density, I_{i}, and electronic current density, I_{e}, in the membrane are opposite; that is if, for example, $I_{\mathrm{i}} < 0$ and $I_{\mathrm{e}} > 0$, then it can be shown that $\mu^{\mathrm{I}}_{\mathrm{O}_2} > \mu^{\mathrm{membrane}}_{\mathrm{O}_2}(x) > \mu^{\mathrm{II}}_{\mathrm{O}_2}$ where $\mu^{\mathrm{I}}_{\mathrm{O}_2}$ and $\mu^{\mathrm{II}}_{\mathrm{O}_2}$ are the chemical potentials of O_2 in the gas phases at the two electrodes, I (cathode) and II (anode), respectively, and $\mu^{\mathrm{membrane}}_{\mathrm{O}_2}(x)$ is the chemical potential of oxygen in the membrane (which is a function of position, x) [6,7]. That is, under these conditions of ionic and electronic currents, the $\mu^{\mathrm{membrane}}_{\mathrm{O}_2}(x)$ is bounded by the respective values at the two electrodes (in the gas phases). A single SOFC satisfies these criteria concerning the directions of current [6]. Thus, in a *single* SOFC, the $\mu^{\mathrm{membrane}}_{\mathrm{O}_2}(x)$ is bounded, and the membrane remains stable as long it is stable in both electrode atmospheres (in both, $\mu^{\mathrm{I}}_{\mathrm{O}_2}$ and $\mu^{\mathrm{II}}_{\mathrm{O}_2}$).

If, however, the directions of ionic and electronic currents are the same; that is if $I_{\mathrm{i}} < 0$ and $I_{\mathrm{e}} < 0$, then it can be shown that the chemical potential of O_2 in the membrane, $\mu^{\mathrm{membrane}}_{\mathrm{O}_2}(x)$, need not be bounded by the respective values at the two electrodes, $\mu^{\mathrm{I}}_{\mathrm{O}_2}$ and $\mu^{\mathrm{II}}_{\mathrm{O}_2}$, and can lie outside the range [6,7]. The relative values of transport parameters play a key role in dictating the $\mu^{\mathrm{membrane}}_{\mathrm{O}_2}(x)$. Instabilities can set in if the $\mu^{\mathrm{membrane}}_{\mathrm{O}_2}(x)$ is very low such that membrane decomposition can occur, and/or if the $\mu^{\mathrm{membrane}}_{\mathrm{O}_2}(x)$ is very large, in which case local cracking/delamination can occur. A voltage-driven oxygen separation device satisfies these criteria concerning the directions of currents. Under such conditions, the $\mu^{\mathrm{membrane}}_{\mathrm{O}_2}(x)$ can lie outside of the $(\mu^{\mathrm{I}}_{\mathrm{O}_2}, \mu^{\mathrm{II}}_{\mathrm{O}_2})$ range, and electrolyte stability can be compromised. Indeed, experimental evidence on the failure of electrolyte membranes in voltage-driven oxygen pumps has been documented and this phenomenon can present significant design and life-related challenges for voltage-driven oxygen separation systems [4,6].

1.2. Basis for solid oxide fuel cell (SOFC) stack degradation

During the operation of an SOFC or a SOFC stack, the flux of oxygen ions in a cell occurs from the cathode to the anode, which means current due to oxygen ion transport through the cell flows from the anode to the cathode (using the usual definition of a positive current). Also, under normal operating conditions, the cathode is at a higher electric potential compared to the anode. Thus, electron transport *through* the cell, however small (due to low electronic conductivity of the membrane), occurs from the anode to the cathode (or electron hole transport from the cathode to the anode), which means electronic current (as a positive current) through the cell flows from the cathode to the anode. Thus, under normal operating conditions, the signs of the ionic and the electronic currents are opposite, and the $\mu^{\mathrm{membrane}}_{\mathrm{O}_2}(x)$ is bounded by the respective values at the two electrodes [6,7]. If, however, under SOFC stack operating conditions, one of the cells has a higher resistance and exhibits a negative voltage, the direction of the ionic current remains the same, but that of electrons through the cell reverses. In such a cell, both the ionic and

electronic currents are in the same direction. In such a cell, the $\mu_{O_2}^{membrane}(x)$ can lie outside of the $(\mu_{O_2}^{I}, \mu_{O_2}^{II})$ range, and this can lead to cell degradation, and subsequent stack degradation. This is the basic premise of the model, which is described in what follows.

2. Mechanism of cell and stack degradation

Fig. 3 shows a schematic representation of a fuel cell with porous electrodes. The interfaces (boundaries) I and II are those corresponding to the porous cathode/electrolyte and porous anode/electrolyte interfaces, respectively. The interfacial regions (or interfaces) referred to here extend a distance δ into the electrolyte from these boundaries. It is understood that $\delta \ll \ell$. The membrane thickness, ℓ, refers to the thickness of the electrolyte. Fig. 4 shows a simplified equivalent circuit for a fuel cell by incorporating electrode/electrolyte interfaces [6]. The equivalent circuit represents the region of the cell between the electrolyte/electrode (cathode and anode) interfaces (between I and II in Fig. 3). Thus, the equivalent circuit does not include concentration polarization associated with gas transport through porous electrodes. It also does not include part of the activation polarization—that part associated with the extended electrochemical zones into the porous electrodes [10,11]. Thus, the sum of the three emfs equals the open circuit voltage (OCV) minus voltage loss associated with the two concentration polarization terms, and parts of the activation polarization associated with the extended zones into the porous electrodes.

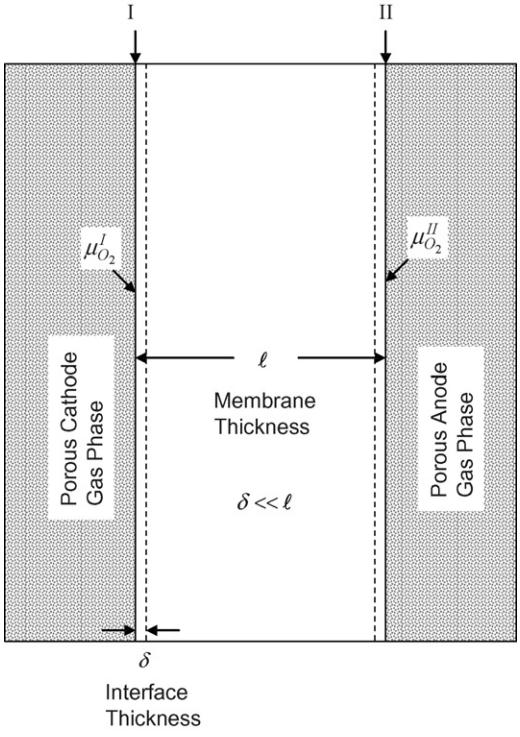

Fig. 3. A schematic representation of a fuel cell showing porous electrodes. The dense electrolyte membrane is of thickness ℓ, and interfacial regions in the electrolyte, at the electrode/electrolyte interfaces are of thickness δ, where $\delta \ll \ell$.

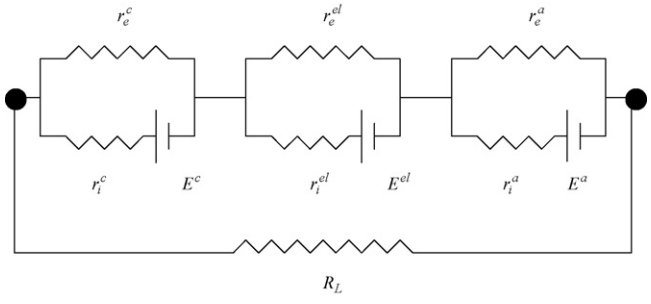

Fig. 4. An equivalent circuit for a solid oxide fuel cell (SOFC) using internal emf sources.

The use of resistances tacitly assumes that for any given region (bulk or interfacial), the transport properties are constant—independent of position and local oxygen chemical potential. In general, transport properties are functions of chemical potential of oxygen (as point defect and electronic species concentrations depend upon oxygen nonstoichiometry, which depends on oxygen chemical potential). Unfortunately, these dependencies are rarely known with sufficient accuracy to allow for a quantitative and experimentally verifiable description of transport processes. And even if known, it is often not possible to develop a simple analytical model and one is forced to numerical calculations. Such an approach is deemed unsatisfactory for elucidating the basic concepts of the model. For this reason, properties are assumed here to be independent of local chemical potential for any given region (interfacial or bulk). Such a simplification only alters the details—not the general, broader conclusions [6].

In what follows, concentration polarization is assumed to be negligible for simplicity, and the activation polarization associated with the extended electrode zones is also neglected. Note the use of internal emfs for interfaces instead of the often-used capacitors [6,12]. The filled circles at the end indicate that the equivalent circuit comprises all circuit elements inside of the filled circles. Note also that transport across the two electrode/electrolyte interfaces is described in terms of two parameters—resistance to ion transport and resistance to electron transport. Thus, the area specific resistances across the cathode/electrolyte interface are given by; r_i^c: ionic charge transfer resistance at the cathode/electrolyte interface, and r_e^c: electronic charge transfer resistance at the cathode/electrolyte interface. The ionic charge transfer resistance, r_i^c, is expected to exhibit thermally activated behavior and is often describable by a phenomenological equation such as the Butler-Volmer equation. That is, for example, the exchange current density at the cathode, i_o^c, will be inversely proportional to r_i^c. The electronic charge transfer resistance, r_e^c, may also exhibit some sort of temperature dependence, and may depend upon the local band structure. The emf across the cathode/electrolyte interface is given by E^c, which is a measure of $\Delta\mu_{O_2}$ across the interface. For the anode/electrolyte interface, the corresponding parameters are r_i^a, r_e^a and E^a. Finally, the respective parameters across the electrolyte are r_i^{el}, r_e^{el}, and E^{el}. The r_i^{el} and r_e^{el} are given, respectively by $\rho_i^{el}\ell$ and $\rho_e^{el}\ell$ where ρ_i^{el} is the ionic resistivity of the membrane and ρ_e^{el} is the electronic resistivity of the membrane. Both ρ_i^{el} and ρ_e^{el} are expected to depend upon the temperature and

μ_{O_2} through appropriate defect equilibria, which are functions of the defect structure, composition and temperature. However, as stated earlier, in what follows, ρ_i^{el} and ρ_e^{el} are assumed to be independent of μ_{O_2} and thus also independent of position.

For SOFC in most cases, except perhaps ceria-based, the electronic resistances are much greater than the ionic resistances; that is, $r_e^{el} \gg r_i^c, r_i^{el}, r_i^a$ and/or $r_e^c \gg r_i^c, r_i^{el}, r_i^a$, and/or $r_e^a \gg r_i^c, r_i^{el}, r_i^a$. In steady state, the ionic current density, I_i, and the electronic current density, I_e, through the three elements of the cell; namely, cathode/electrolyte interface, electrolyte, and anode/electrolyte interface, are uniform [6].[1] The externally applied load, R_L (in $\Omega\,cm^2$)[2] determines the two current densities, which are given by [6]

$$I_i = -\frac{E(R_e + R_L)}{R_L R_e + R_i(R_e + R_L)} \tag{5}$$

and

$$I_e = \frac{E R_L}{R_L R_e + R_i(R_e + R_L)} \tag{6}$$

where

$$E = E^c + E^{el} + E^a \tag{7}$$

$$R_i = r_i^c + r_i^{el} + r_i^a \tag{8}$$

and

$$R_e = r_e^c + r_e^{el} + r_e^a \tag{9}$$

In Eqs. (5)–(7), E denotes the open circuit voltage minus concentration polarization and possible activation polarization associated with the extended electrode zones. The emfs E^c, E^{el}, and E^a, depend upon the various resistances including the load, and E [6]. In what follows, it is assumed that concentration polarizations and activation polarizations associated with extended electrode zones are small, and thus E is assumed to be the same as the Nernst voltage, E_0 (since $R_e \gg R_i$). Again, this only changes the details—not the general conclusions.

2.1. Chemical potential as a function of current densities and specific resistances

It can be shown that the chemical potential of oxygen in the *electrolyte* just inside the cathode/electrolyte interface, $\mu_{O_2}^c$, is given by [6]

$$\mu_{O_2}^c = \mu_{O_2}^I + 4e(r_i^c I_i - r_e^c I_e) \tag{10}$$

where the μ_{O_2}'s are defined on a per molecule basis, or

$$\mu_{O_2}^c = \mu_{O_2}^I + 4F(r_i^c I_i - r_e^c I_e) \tag{11}$$

where F is the Faraday constant and the μ_{O_2}'s are defined on a per mole basis. Similarly, the chemical potential of oxygen in the electrolyte just inside the anode/electrolyte interface, $\mu_{O_2}^a$, is given by [6]

$$\mu_{O_2}^a = \mu_{O_2}^{II} - 4e(r_i^a I_i - r_e^a I_e) \tag{12}$$

on a per molecule basis, or

$$\mu_{O_2}^a = \mu_{O_2}^{II} - 4F(r_i^a I_i - r_e^a I_e) \tag{13}$$

on a per mole basis. In what follows, whenever e is used for the electrical charge, all μ's and $\tilde{\mu}$'s are on a per species (atom, molecule, ion, electron) basis; and whenever F is used, all μ's and $\tilde{\mu}$'s are on a molar basis. In terms of the parameters defined in Eqs. (5)–(9) and the cell voltage, V_C, the above equations may also be written as

$$\mu_{O_2}^c = \mu_{O_2}^I + 4e\left\{\frac{r_i^c(V_C - E)}{R_i} - \frac{r_e^c V_C}{R_e}\right\} \tag{14}$$

and

$$\mu_{O_2}^a = \mu_{O_2}^{II} - 4e\left\{\frac{r_i^a(V_C - E)}{R_i} - \frac{r_e^a V_C}{R_e}\right\} \tag{15}$$

Similarly, the chemical potential of O_2 in the membrane as a function of position, x, namely $\mu_{O_2}^{membrane}(x)$, is given by

$$\mu_{O_2}^{membrane}(x) = \mu_{O_2}^c + \frac{x}{\ell}(\mu_{O_2}^a - \mu_{O_2}^c) \tag{16}$$

From Eqs. (14) and (15), the oxygen pressures in the electrolyte, just inside the electrode/electrolyte interfaces are given by

$$p_{O_2}^c = p_{O_2}^I \exp\left[\frac{4e}{k_B T}\left\{\frac{r_i^c(V_C - E)}{R_i} - \frac{r_e^c V_C}{R_e}\right\}\right] \tag{17}$$

and

$$p_{O_2}^a = p_{O_2}^{II} \exp\left[-\frac{4e}{k_B T}\left\{\frac{r_i^a(V_C - E)}{R_i} - \frac{r_e^a V_C}{R_e}\right\}\right] \tag{18}$$

where k_B is the Boltzmann constant, T is the absolute temperature, and the ideal gas law is assumed. From Eqs. (10) or (14) and (12) or (15), it is immediately apparent that in general the chemical potentials of oxygen just inside the solid electrolyte, across the interfaces, must be different from the corresponding values in the respective gas phases. That is, we must have $\mu_{O_2}^c \neq \mu_{O_2}^I$ and $\mu_{O_2}^a \neq \mu_{O_2}^{II}$, when $\mu_{O_2}^I \neq \mu_{O_2}^{II}$ and/or when an external voltage is applied, regardless of whether the electrodes are reversible or not. It has been a common practice to assume that if the polarization losses are negligible (reversible electrodes), then $\mu_{O_2}^c = \mu_{O_2}^I$ and $\mu_{O_2}^a = \mu_{O_2}^{II}$ [9]. However, for this to be the case, the terms in parentheses in Eqs. (10) and (12) will need to be identically zero, which would be a very unusual and a special case—and not a general case. It is for this reason, an abrupt change in μ_{O_2} must occur across both gas–solid interfaces when $\mu_{O_2}^I - \mu_{O_2}^{II} \neq 0$, and as long as there is a finite, nonzero interface thickness, δ, even when the electrodes are reversible. For the reasons stated earlier, the δ must always be greater than zero. Recent work on SOFC with embedded reference electrodes has indeed shown that even at OCV (when electrodes effectively are reversible), there is an abrupt change in μ_{O_2} across electrode/electrolyte interfaces [13]. Also, for the same reasons, the integration limits for obtaining the average of

[1] That is $\nabla\cdot I_i = 0$ and $\nabla\cdot I_e = 0$, or in a one-dimensional case, $dI_i/dx = 0$ and $dI_e/dx = 0$.

[2] Defined as load (Ω) multiplied by actual electrode area (cm^2).

any μ_{O_2}-dependent property of the membrane are from $\mu^{c}_{O_2}$ and $\mu^{a}_{O_2}$, and not from $\mu^{I}_{O_2}$ and $\mu^{II}_{O_2}$. If $\mu^{I}_{O_2}$ and $\mu^{II}_{O_2}$ are used as integration limits, the error may be particularly large for relatively thin membranes, such as those in electrode-supported cells.

For an SOFC operating normally, $I_i < 0$ and $I_e > 0$. Thus, Eqs. (10) and (12), respectively become

$$\mu^{c}_{O_2} = \mu^{I}_{O_2} + 4e(r^{c}_{i} I_i - r^{c}_{e} I_e) = \mu^{I}_{O_2} - 4e(r^{c}_{i}|I_i| + r^{c}_{e}|I_e|) \tag{19}$$

and

$$\mu^{a}_{O_2} = \mu^{II}_{O_2} - 4e(r^{a}_{i} I_i - r^{a}_{e} I_e) = \mu^{II}_{O_2} + 4e(r^{a}_{i}|I_i| + r^{a}_{e}|I_e|) \tag{20}$$

In terms of the cell voltage, this implies $0 \le V_C \le E$. Under such conditions, note from Eqs. (14), (15), (17)–(20) that $\mu^{c}_{O_2} < \mu^{I}_{O_2}$ (and $p^{c}_{O_2} < p^{I}_{O_2}$) and $\mu^{a}_{O_2} > \mu^{II}_{O_2}$ (and $p^{a}_{O_2} > p^{II}_{O_2}$), and it can be readily shown that $\mu^{c}_{O_2} > \mu^{a}_{O_2}$ ($p^{c}_{O_2} > p^{a}_{O_2}$) [6]. Thus, the chemical potential of oxygen within the electrolyte, $\mu^{membrane}_{O_2}(x)$, is bounded by the values in the gas phases just outside electrolyte/electrode interfaces. It is for this reason, it was stated earlier that the $\mu^{membrane}_{O_2}(x)$ is bounded by the values at the two electrodes (i.e. values in the gas phases outside the membrane), that is $\mu^{I}_{O_2} > \mu^{membrane}_{O_2}(x) > \mu^{II}_{O_2}$, and *not* $\mu^{I}_{O_2} \ge \mu^{membrane}_{O_2}(x) \ge \mu^{II}_{O_2}$ [14].

2.2. Electrode polarization loss and $\Delta\mu^{interface}_{O_2}$

Eqs. (19) and (20) can be used to estimate the change of μ_{O_2} across the interfaces as a function of polarization. If the electrolyte is predominantly an ionic conductor with very low electronic conductivity and if the electrodes are highly active with negligible polarization losses, the implication is that at a finite nonzero current $|I_i|r^{c}_{i} \to 0$ (negligible cathode activation polarization) and $|I_i|r^{a}_{i} \to 0$ (negligible anode activation polarization). This of course means $r^{c}_{i} \to 0$ and $r^{a}_{i} \to 0$. For these conditions (that is, reversible electrodes) Eqs. (19) and (20), respectively become

$$\mu^{c}_{O_2} = \mu^{I}_{O_2} + 4e(r^{c}_{i} I_i - r^{c}_{e} I_e) \approx \mu^{I}_{O_2} - 4e r^{c}_{e}|I_e| \tag{21}$$

and

$$\mu^{a}_{O_2} = \mu^{II}_{O_2} - 4e(r^{a}_{i} I_i - r^{a}_{e} I_e) \approx \mu^{II}_{O_2} + 4e r^{a}_{e}|I_e| \tag{22}$$

It is clear from Eqs. (21) and (22) that in general $\mu^{c}_{O_2} \ne \mu^{I}_{O_2}$ (and in this case $\mu^{c}_{O_2} < \mu^{I}_{O_2}$) and $\mu^{a}_{O_2} \ne \mu^{II}_{O_2}$ (and in this case $\mu^{a}_{O_2} > \mu^{II}_{O_2}$) since one can readily have $r^{c}_{e}|I_e| > 0$ and $r^{a}_{e}|I_e| > 0$, even though electrodes are reversible.

As was demonstrated recently, accurate measures of cathode and anode polarizations (as rates of energy loss in the form of heat) are given by $|I\eta^{c}_{act}| = I^2_i r^{c}_{i} + I^2_e r^{c}_{e}$ and $|I\eta^{a}_{act}| = I^2_i r^{a}_{i} + I^2_e r^{a}_{e}$ in W cm^{-2}, respectively, where I is the measured current (density) [6]. These equations *define* the cathode and anode activation polarizations, η^{c}_{act} and η^{a}_{act}, respectively. When $R_e \gg R_i$, at finite, nonzero current in the external circuit, there is virtually no difference between the conventionally defined polarization and that described in terms of the rate of energy loss as heat. However, at OCV, there is a significant difference between the two, as elaborated in [6].

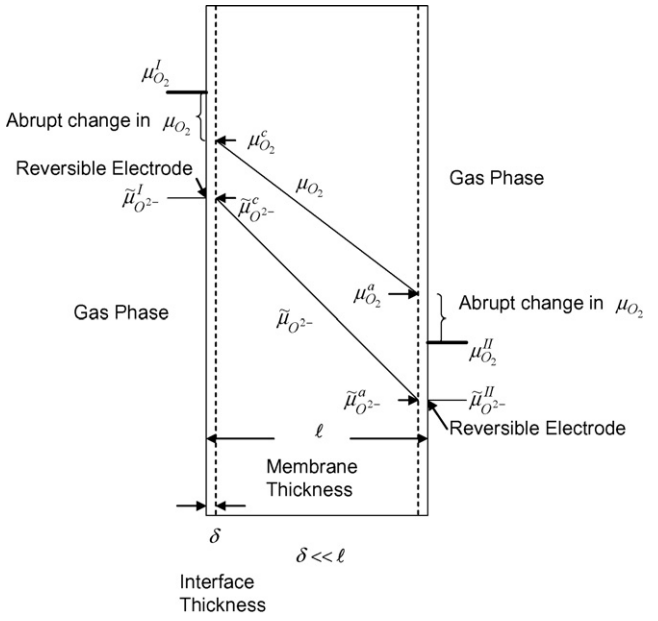

Fig. 5. A schematic representation of a fuel cell under load (load is not shown) with a finite current passing through the cell. It is assumed that the electrodes are very active with negligible polarizations (reversible electrodes). Thus, $\tilde{\mu}^{I}_{O^{2-}} \approx \tilde{\mu}^{c}_{O^{2-}}$ and $\tilde{\mu}^{II}_{O^{2-}} \approx \tilde{\mu}^{a}_{O^{2-}}$. Yet there are abrupt changes in the chemical potential of oxygen, μ_{O_2}, across the two interfaces. That is, note that $\mu^{I}_{O_2} \ne \mu^{c}_{O_2}$ and $\mu^{II}_{O_2} \ne \mu^{a}_{O_2}$. Thus, low polarization losses at the electrodes does not mean equilibration of the μ_{O_2}, as has been commonly assumed [9]. It is assumed here that $\delta \ll \ell$ and that δ is on the order of angstroms.

The overpotential losses can be small (low activation polarization), and still $\Delta\mu^{interface}_{O_2} \ne 0$. This is because low polarization in predominantly ionic conductors means $\varepsilon > I^2_i r^{c,a}_{i} \gg I^2_e r^{c,a}_{e} > 0$ where ε is a positive quantity, however small. This condition can be satisfied, and yet one has $r^{c}_{e}|I_e| \gg r^{c}_{i}|I_i| \ge 0$ and $r^{a}_{e}|I_e| \gg r^{a}_{i}|I_i| \ge 0$. When the polarization is negligible, the implication is that $\tilde{\mu}^{I}_{O^{2-}} \approx \tilde{\mu}^{c}_{O^{2-}}$ and $\tilde{\mu}^{II}_{O^{2-}} \approx \tilde{\mu}^{a}_{O^{2-}}$. However, as described here and shown previously [6], one still has $\mu^{c}_{O_2} \ne \mu^{I}_{O_2}$ (and in this case $\mu^{c}_{O_2} < \mu^{I}_{O_2}$) and $\mu^{a}_{O_2} \ne \mu^{II}_{O_2}$ (and in this case $\mu^{a}_{O_2} > \mu^{II}_{O_2}$). This is shown schematically in Fig. 5.

2.3. A numerical example

For the purposes of illustration, let us consider the following numerical example. The temperature is assumed to be 800 °C or 1073 K. The open circuit voltage is 1.0 V, the cell is being operated at 0.7 V, and the net current density is 1 A cm^{-2}. This means the net ionic area specific resistance (ASR or R_i) of the cell is 0.3 Ω cm^2, which is also the measured cell specific resistance, $R_N = R_i R_e/(R_i + R_e)$, since $R_e \gg R_i$. Let us assume that the cathode exhibits very low polarization, characterized by a very low r^{c}_{i}. We will assume $r^{c}_{i} = 0.01\ \Omega\,\text{cm}^2$. The electronic charge transfer resistance at the cathode is assumed as $r^{c}_{e} = 10^3\ \Omega\,\text{cm}^2$, which is five orders of magnitude greater than the ionic charge transfer resistance, r^{c}_{i}. The oxygen partial pressure at the cath-

ode is $p^{\mathrm{I}}_{\mathrm{O}_2} = 0.21$ atm. Now, $|I_\mathrm{i}| \approx 1$, where I is the measured current density (1 A cm^{-2}), since $I_\mathrm{e} \ll |I_\mathrm{i}|$. It is readily seen that

$$\tilde{\mu}^{\mathrm{I}}_{\mathrm{O}^{2-}} - \tilde{\mu}^{\mathrm{c}}_{\mathrm{O}^{2-}} = 2Fr^{\mathrm{c}}_\mathrm{i}|I_\mathrm{i}| = 2Fr^{\mathrm{c}}_\mathrm{i}I \tag{23}$$

For the values selected, $\tilde{\mu}^{\mathrm{I}}_{\mathrm{O}^{2-}} - \tilde{\mu}^{\mathrm{c}}_{\mathrm{O}^{2-}} = 0.02F$ (J mol^{-1}). This represents an abrupt change in the electrochemical potential of oxygen ions across the cathode/electrolyte interface—a measure of the traditional definition of cathode activation polarization. Note that the smaller the $r^{\mathrm{c}}_\mathrm{i}$, the lower is this step change in electrochemical potential, $\tilde{\mu}_{\mathrm{O}^{2-}}$, the lower is the cathode activation polarization, the more reversible is the cathode.[3] Let us now further assume that $I_\mathrm{e} = 7\times10^{-5}$ A cm^{-2} (which means $R_\mathrm{e} = 10^4\ \Omega\,\mathrm{cm}^2$). It is easily seen that $\varphi^{\mathrm{I}} - \varphi^{\mathrm{c}} = r^{\mathrm{c}}_\mathrm{e}I_\mathrm{e}$, where $\varphi = -\tilde{\mu}_\mathrm{e}/e$ (or $\varphi = -\tilde{\mu}_\mathrm{e}/F$ if $\tilde{\mu}_\mathrm{e}$ is given on a per mole basis). For the values selected, the voltage drop across the cathode/electrolyte interface, $\varphi^{\mathrm{I}} - \varphi^{\mathrm{c}}$, is 0.07 V.

Finally, the $\mu^{\mathrm{I}}_{\mathrm{O}_2} - \mu^{\mathrm{c}}_{\mathrm{O}_2}$ difference using Eq. (19) is given by

$$\mu^{\mathrm{I}}_{\mathrm{O}_2} - \mu^{\mathrm{c}}_{\mathrm{O}_2} = 4F(r^{\mathrm{c}}_\mathrm{i}|I_\mathrm{i}| + r^{\mathrm{c}}_\mathrm{e}I_\mathrm{e}) = 4F(r^{\mathrm{c}}_\mathrm{i}I + r^{\mathrm{c}}_\mathrm{e}I_\mathrm{e}) \tag{24}$$

(using the molar basis). Again, the key point to note is that the first term in the parenthesis in Eq. (24) is a measure of cathode activation polarization as conventionally defined. This term may be negligible compared to the second term when electrodes are highly active. For the case considered, the first term in the parenthesis is 0.01 V (for $r^{\mathrm{c}}_\mathrm{i} = 0.01\ \Omega\,\mathrm{cm}^2$) while the second term is 0.07 V. Thus, from the above equation, note that $\mu^{\mathrm{I}}_{\mathrm{O}_2} - \mu^{\mathrm{c}}_{\mathrm{O}_2} = 0.32F$ (J mol^{-1}). That is, $\tilde{\mu}^{\mathrm{I}}_{\mathrm{O}^{2-}} - \tilde{\mu}^{\mathrm{c}}_{\mathrm{O}^{2-}}$ is negligible (negligible conventionally defined cathode activation polarization[4] or essentially a reversible cathode), but $\mu^{\mathrm{I}}_{\mathrm{O}_2} - \mu^{\mathrm{c}}_{\mathrm{O}_2}$ is substantial. Fig. 5 schematically shows the abrupt drop in μ_{O_2} across the cathode/electrolyte interface. The corresponding $p^{\mathrm{c}}_{\mathrm{O}_2}$ is given by $p^{\mathrm{c}}_{\mathrm{O}_2} \approx 6.6\times10^{-3}$ atm. That is, there is an abrupt change in p_{O_2} across the interface.

As stated earlier, activation polarization loss at the cathode, defined as heat loss per unit time per unit area is given by $|I\eta^{\mathrm{c}}_{\mathrm{act}}| = r^{\mathrm{c}}_\mathrm{i}I^2_\mathrm{i} + r^{\mathrm{c}}_\mathrm{e}I^2_\mathrm{e}$ [6]. For the values selected here:

$$\begin{aligned}|I\eta^{\mathrm{c}}_{\mathrm{act}}| &= r^{\mathrm{c}}_\mathrm{i}I^2_\mathrm{i} + r^{\mathrm{c}}_\mathrm{e}I^2_\mathrm{e} = 0.01\times1^2 + 10^3\times(7\times10^{-5})^2\\ &= 0.01 + 4.9\times10^{-6}\ \mathrm{W\,cm^{-2}}\end{aligned} \tag{25}$$

For the assumed values, the ionic part of the polarization is 0.01 W cm^{-2}, which is rather small. Note that polarization loss associated with electronic charge transfer is even much smaller (as expected due to large $r^{\mathrm{c}}_\mathrm{e}$). However, $r^{\mathrm{c}}_\mathrm{e}I_\mathrm{e}$ is not insignificant, and does indeed have a large effect on the change of μ_{O_2} across the interfaces, as described here.

If the same cell is at OCV, then no current flows through the external circuit and $I_\mathrm{i} + I_\mathrm{e} = 0$ or $I_\mathrm{e} = -I_\mathrm{i}$, which is given by 10^{-4} A cm^{-2}. The corresponding $\tilde{\mu}^{\mathrm{I}}_{\mathrm{O}^{2-}} - \tilde{\mu}^{\mathrm{c}}_{\mathrm{O}^{2-}} \approx 0$. However, the corresponding $\mu^{\mathrm{I}}_{\mathrm{O}_2} - \mu^{\mathrm{c}}_{\mathrm{O}_2} = \Delta\mu^{\mathrm{interface}}_{\mathrm{O}_2} \neq 0$ and is given by

$$\begin{aligned}\mu^{\mathrm{I}}_{\mathrm{O}_2} - \mu^{\mathrm{c}}_{\mathrm{O}_2} &= 4F(r^{\mathrm{c}}_\mathrm{i}|I_\mathrm{i}| + r^{\mathrm{c}}_\mathrm{e}I_\mathrm{e}) = 4F(r^{\mathrm{c}}_\mathrm{i}I_\mathrm{e} + r^{\mathrm{c}}_\mathrm{e}I_\mathrm{e}) \approx 4FI_\mathrm{e}r^{\mathrm{c}}_\mathrm{e}\\ &= 0.4F\ (\mathrm{J\,mol^{-1}})\end{aligned}$$

That is, there is a large change in μ_{O_2} across the cathode/electrolyte interface even at OCV when the cathode is perfectly reversible. For the aforementioned reasons, the commonly made assumption of the equilibration of chemical potential of oxygen across the interfaces is not valid, even when the electrodes behave reversibly [9]. As stated earlier, experimental measurements at OCV are in accord with this expectation [13].

2.4. Cell in a stack behaving normally

To recap, when a cell is behaving normally, the ionic and the electronic currents are in the opposite directions and the cell voltage, V_C, is positive. In such a case, the $\mu^{\mathrm{membrane}}_{\mathrm{O}_2}(x)$, is bounded by $(\mu^{\mathrm{I}}_{\mathrm{O}_2}, \mu^{\mathrm{II}}_{\mathrm{O}_2})$. Fig. 6(a) shows a schematic variation of the $\mu^{\mathrm{membrane}}_{\mathrm{O}_2}(x)$ with position for this case.

2.5. Cell in a stack behaving abnormally

Consider now a case wherein one cell in a stack has a high resistance, and is operating such that voltage across the cell is negative. Then we have $I_\mathrm{i} < 0$ and $I_\mathrm{e} < 0$. Under such conditions, Eqs. (10) and (12) become

$$\mu^{\mathrm{c}}_{\mathrm{O}_2} = \mu^{\mathrm{I}}_{\mathrm{O}_2} + 4e(r^{\mathrm{c}}_\mathrm{i}I_\mathrm{i} - r^{\mathrm{c}}_\mathrm{e}I_\mathrm{e}) = \mu^{\mathrm{I}}_{\mathrm{O}_2} - 4e(r^{\mathrm{c}}_\mathrm{i}|I_\mathrm{i}| - r^{\mathrm{c}}_\mathrm{e}|I_\mathrm{e}|) \tag{26}$$

and

$$\mu^{\mathrm{a}}_{\mathrm{O}_2} = \mu^{\mathrm{II}}_{\mathrm{O}_2} - 4e(r^{\mathrm{a}}_\mathrm{i}I_\mathrm{i} - r^{\mathrm{a}}_\mathrm{e}I_\mathrm{e}) = \mu^{\mathrm{II}}_{\mathrm{O}_2} + 4e(r^{\mathrm{a}}_\mathrm{i}|I_\mathrm{i}| - r^{\mathrm{a}}_\mathrm{e}|I_\mathrm{e}|) \tag{27}$$

An important point to note is that even in a cell behaving abnormally, the ionic current density is almost the same as the other cells behaving normally (since $|I_\mathrm{i}| \gg |I_\mathrm{e}|$ and the net current is the same through all series-connected cells). This also means the rates of gas fluxes (fuel and oxidant) through the porous electrodes towards the electrode/electrolyte interfaces to sustain the current density are identical in all cells. This further means that concentration polarizations are also the same in all cells, each cathode/electrolyte interface is exposed to the same chemical potential (partial pressure) of oxygen, $\mu^{\mathrm{I}}_{\mathrm{O}_2}$ ($p^{\mathrm{I}}_{\mathrm{O}_2}$), and each anode/electrolyte interface is exposed to the same chemical potential (partial pressure) of oxygen, $\mu^{\mathrm{II}}_{\mathrm{O}_2}$ ($p^{\mathrm{II}}_{\mathrm{O}_2}$). Thus, even when a cell in a stack is behaving abnormally (higher resistance), the oxygen partial pressures just outside the electrode/electrolyte interfaces into the electrodes are unchanged and oxidation of nickel is not expected unless the cell membrane has physically cracked.

In terms of the cell voltage, abnormal cell behavior implies $V_\mathrm{C} < 0 < E$. Note that in such a case, the relative magnitudes of $\mu^{\mathrm{c}}_{\mathrm{O}_2}$ and $\mu^{\mathrm{a}}_{\mathrm{O}_2}$ depend upon the relative magnitudes of $r^{\mathrm{c}}_\mathrm{i}|I_\mathrm{i}|$ and $r^{\mathrm{c}}_\mathrm{e}|I_\mathrm{e}|$ and $r^{\mathrm{a}}_\mathrm{i}|I_\mathrm{i}|$ and $r^{\mathrm{a}}_\mathrm{e}|I_\mathrm{e}|$, respectively (or relative magnitudes

[3] If $r^{\mathrm{c}}_\mathrm{i} \to 0$, one has $\tilde{\mu}^{\mathrm{I}}_{\mathrm{O}^{2-}} \approx \tilde{\mu}^{\mathrm{c}}_{\mathrm{O}^{2-}}$ (as shown schematically in Fig. 5), and the cathode is reversible.

[4] Since $|I_\mathrm{i}|r^{\mathrm{c}}_\mathrm{i}$ is small and $I^2_\mathrm{i}r^{\mathrm{c}}_\mathrm{i} \gg I^2_\mathrm{e}r^{\mathrm{c}}_\mathrm{e}$, it is understood that for the case considered here, polarization is negligible—regardless of the definition used (voltage loss or rate of energy loss as heat per unit area) [6].

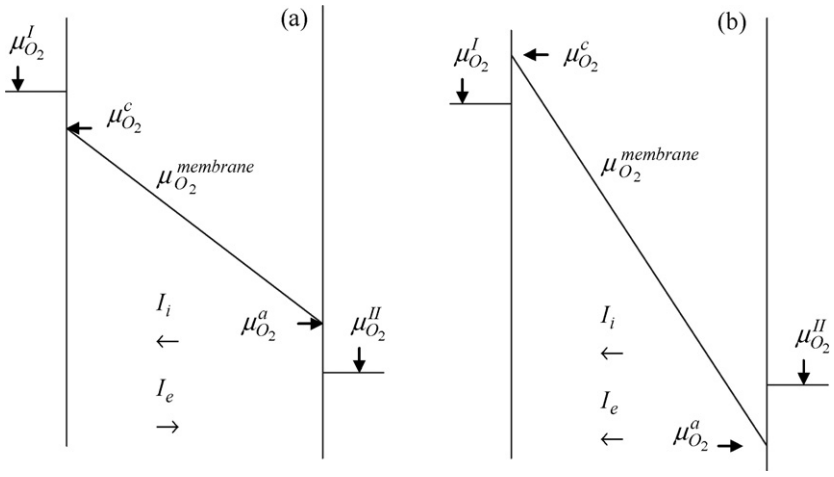

Fig. 6. A schematic representation of $\mu_{O_2}^{membrane}(x)$ as a function of position: (a) an SOFC operating normally. The $\mu_{O_2}^{membrane}(x)$ is in the $(\mu_{O_2}^{I}, \mu_{O_2}^{II})$ range (bounded). I_i and I_e in opposite directions. (b) An SOFC operating abnormally—negative voltage across the cell. The $\mu_{O_2}^{membrane}(x)$ is outside the $(\mu_{O_2}^{I}, \mu_{O_2}^{II})$ range (not bounded). I_i and I_e in the same direction. The 'interface' thicknesses are not shown in the figure since $\delta \ll \ell$.

of the terms in parentheses in Eqs. (14) and (15)). Note also that under such conditions, depending upon the relative magnitudes of $r_i^c|I_i|$ and $r_e^c|I_e|$ and $r_i^a|I_i|$ and $r_e^a|I_e|$, the $\mu_{O_2}^{membrane}(x)$ can lie outside of the $(\mu_{O_2}^{I}, \mu_{O_2}^{II})$ range.

Consider a cell in a SOFC stack operating abnormally, that is $V_C < 0$. Let us also assume that cathode and anode activation polarizations are negligible (reversible electrodes). This implies $r_i^c/R_i \ll 1$ and $r_i^a/R_i \ll 1$. Then Eqs. (14) and (15) become, respectively,

$$\mu_{O_2}^{c} \approx \mu_{O_2}^{I} - 4e\frac{r_e^c V_C}{R_e} = \mu_{O_2}^{I} + 4e\frac{r_e^c|V_C|}{R_e} > \mu_{O_2}^{I} \tag{28}$$

and

$$\mu_{O_2}^{a} \approx \mu_{O_2}^{II} + 4e\frac{r_e^a V_C}{R_e} = \mu_{O_2}^{II} - 4e\frac{r_e^a|V_C|}{R_e} < \mu_{O_2}^{II} \tag{29}$$

Fig. 6(b) shows a schematic variation of $\mu_{O_2}^{membrane}(x)$ (not bounded) as a function of position for this case. Let us now examine two limiting cases. In one case, we will assume that much of the *electronic* resistance is associated with the cathode/electrolyte interface; that is, $r_e^c \gg r_e^a, r_e^{el}$. This may occur, for example, if an electronically insulating phase forms at the cathode/electrolyte interface during processing and/or operation. In such a case, $r_e^c/R_e \approx 1$, and Eq. (28) reduces to

$$\mu_{O_2}^{c} \approx \mu_{O_2}^{I} + 4e|V_C| \tag{30}$$

Since $\mu_{O_2}^{I} = \mu_{O_2}^{\circ} + k_B T \ln p_{O_2}^{I}$ (assuming the ideal gas law) where $\mu_{O_2}^{\circ}$ is the standard state gas phase oxygen chemical potential and $p_{O_2}^{I}$ is the oxygen partial pressure at the cathode (gas phase), Eq. (30) gives

$$p_{O_2}^{c} \approx p_{O_2}^{I} \exp\left[\frac{4e|V_C|}{k_B T}\right] \tag{31}$$

which shows that $p_{O_2}^{c} > p_{O_2}^{I}$. If $p_{O_2}^{c}$ is sufficiently large, cracking/delamination at the cathode is likely. In order to estimate the possible magnitude of $p_{O_2}^{c}$, numerical estimates are presented in what follows for assumed values of parameters.

Let the operating temperature be 800 °C (1073 K). Also, let us assume that $V_C = -0.2$ V. That is, while the rest of the cells in a stack are behaving normally, voltage across one cell behaving abnormally is −0.2 V. Then with air as the oxidant ($p_{O_2}^{I} = 0.21$ atm), the estimated $p_{O_2}^{c} \approx 1200$ atm (∼17,000 p.s.i. or ∼117 MPa), which is an enormous pressure. The calculation shows that even a modest value of $|V_C|$ (with $V_C < 0$) can lead to very large pressures. This pressure develops in the electrolyte, just under the cathode/electrolyte interface. Under such a pressure, delamination of the cathode (or near the cathode region) is inevitable causing further damage to the cell.[5] Post-test examination if the SOFC operation is *voluntarily* interrupted at such a stage (Fortuitously? Because there may be no warning signs in a stack comprising many cells), will reveal the occurrence of cathode delamination. A key point to note is that such delamination of the cathode is likely the result of internal pressure built up as described here, and need not represent inherently bad or poor cathode/electrolyte interface bonding. That is, the observation of a weak (delaminated) cathode/electrolyte interface in post-test or postmortem examination may not necessarily be related to poor firing of the cathode or other such superficial causes. But rather, it is a manifestation of internal pressures generated as described here. Of course once cathode/electrolyte interface has delaminated subsequent degradation will continue to occur and at an accelerated pace. Once the cathode has delaminated, further increase in cell resistance occurs leading to significant local heating, stress development, cracking and subsequent anode destruction by re-oxidation when fuel and oxidant locally mix and react.

In the other limiting case, let us assume that much of the electronic resistance is associated with the anode/electrolyte

[5] Indeed, in the oxygen pumping mode pitting and electrode delamination has been experimentally documented [4].

interface; that is, $r_e^a \gg r_e^c, r_e^{el}$. In such a case, $r_e^a/R_e \approx 1$, and Eq. (29) reduces to

$$\mu_{O_2}^a \approx \mu_{O_2}^{II} - 4e|V_C| \tag{32}$$

The corresponding oxygen partial pressure in the electrolyte close to the anode/electrolyte interface is given by

$$p_{O_2}^a \approx p_{O_2}^{II} \exp\left[-\frac{4e|V_C|}{k_B T}\right] \tag{33}$$

and $p_{O_2}^a < p_{O_2}^{II}$. Let us assume that $p_{O_2}^{II} \approx 10^{-20}$ atm, the oxygen partial pressure in the electrode just outside anode/electrolyte interface in the gas phase. The decomposition potential of zirconia is ~2.3 V at 800 °C (1073 K) or an oxygen partial pressure of $\sim 10^{-44}$ atm [15]. This means for electrolyte decomposition to occur, the $V_C \leq -1.3$ V. Thus, according to this model, the likely degradation mechanism involves the occurrence of electrolyte decomposition just under the anode/electrolyte interface when $r_e^a \gg r_e^c, r_e^{el}$. That is, the mechanism predicts decomposition of the electrolyte just under the anode/electrolyte interface—and not re-oxidation of the anode. Once this occurs, however, cracking could occur allowing fuel and oxidant to locally mix. Then under such conditions, the local oxygen partial pressure will be sufficiently high to oxidize Ni to NiO. Thus, the often-observed re-oxidation of the anode is due to cell degradation by the above-described mechanism leading to local cracking, mixing of fuel and oxidant thus oxidizing nickel, and not as a result of presumably too high an oxygen pressure at high current density causing oxidation of Ni to NiO, as has been often assumed.

The likelihood of delamination at the cathode due to excess pressure build up is greater than electrolyte decomposition at the anode due to too low oxygen partial pressure since the required $|V_C|$ is smaller (with $V_C < 0$). In a large stack, however, either of the situations may occur, and without prior advance notice unless voltages on individual cells are monitored. For example, suppose a stack contains 100 cells, and the stack is operated at 0.7 V cell^{-1} or at 70 V. It would not be hard to imagine a 'bad' cell operating at say −1.4 V, with all other cells operating at 0.7212 V each, for a total of 70 V. The problem is, in the absence of measurement of voltages across each of the cells (or at least small groups of cells), there would be no easy way of identifying the 'bad' cell.

3. Degradation kinetics

Thus far, only the steady state problem has been examined. From the standpoint of applications, an important question concerns the kinetics with which stack degradation occurs, once deviation from the normal behavior (one or more cells in a stack operating at a $V_C < 0$) sets in. As stated earlier, there are a multitude of causes why a cell or a repeat unit may develop a high resistance. The question we wish to address is how long will it require for the cell to fail, where failure is defined as electrode delamination and/or local electrolyte decomposition, once the cell has begun to operate abnormally ($V_C < 0$). In what follows, only the case of cathode delamination by build up of pressure in the electrolyte just inside the cathode/electrolyte interface is addressed. Thus, the question we wish to address is: 'How long will it take to build up the oxygen partial pressure in the electrolyte just under the cathode/electrolyte interface, $p_{O_2}^c$, to a value sufficiently high to delaminate the cathode, once V_C has gone negative?' Unfortunately, the answer to this question depends upon a number of factors/parameters, many of which are not easily accessible. Nevertheless, the fundamental basis for the calculation will be presented here, which should yield some insight into the expected time.

In addition to all transport parameters discussed here, a critical parameter governing the time to reach a given pressure includes the rate of change of local oxygen pressure, p_{O_2}, as a function of the number of moles of O_2 accumulated at the position, n_{O_2}, namely $\partial p_{O_2}/\partial n_{O_2}$. This parameter describes the increase in local oxygen partial pressure when one mole of O_2 is locally 'deposited'. The $n_{O_2}(t)$ describes the net amount of O_2 deposited by transport at the prescribed location, e.g. in the electrolyte just under the cathode/electrolyte interface.

If the material (or the interfacial region) exhibits nonstoichiometry, the relevant parameter may be the 'chemical capacitance', which can also be related to the above-described parameter. The higher the chemical capacitance, the lower will be $\partial p_{O_2}/\partial n_{O_2}$, and the longer will it take to reach a prescribed pressure. A detailed knowledge of the dependence of nonstoichiometry on μ_{O_2}, which is rarely available, is required. An alternative approach involves the assumption of isolated (not connected to the cathode gas phase) pores or voids at the electrode/electrolyte interfaces. In such a case, the higher the pore or the void volume, the lower is $\partial p_{O_2}/\partial n_{O_2}$, and the longer will it take to reach a certain pressure. This was the approach used previously, and will be used here to discuss the kinetics of degradation [3,4].

Let us assume that there exists an isolated pore or a void at the cathode/electrolyte interface just inside the electrolyte, whose volume is given by v_c. In such a case, assuming the ideal gas law,

$$n_{O_2}^c(t) = \frac{p_{O_2}^c(t) v_c}{RT} \tag{34}$$

When $p_{O_2}^c(t)$ exceeds some critical value, $p_{O_2}(\mathrm{cr})$, beyond which electrode delamination can occur (which in turn depends upon fracture mechanical properties such as fracture toughness or fracture energy), cell damage will occur. As described in [4], the cracking is expected to be stable fracture and not rapid fracture. The $n_{O_2}^c(t)$ is given by [3,4]

$$n_{O_2}^c(t) = \lambda \frac{\left| \int_0^t (I_i^c(t') - I_i^{el}(t'))\, dt' \right|}{4F} \tag{35}$$

where $I_i^c(t')$ and $I_i^{el}(t')$ are respectively ionic current densities in the cathode/electrolyte segment of the equivalent circuit at time, t', and the electrolyte segment of the equivalent circuit at time, t', and λ is a geometrical parameter with units of area which is related to the pore size and geometry. Note that in a nonsteady state, $I_i^c(t') \neq I_i^{el}(t') \neq I_i^a(t')$, as discussed in [3,4,6]. The approach to calculations involves writing down mass bal-

ance equations in terms of time dependent ionic and electronic current densities for the three segments of the equivalent circuit subject to Kirchoff's laws and initial conditions, as described in [3] and [4]. From Eqs. (34) and (35), let us write $p^{c}_{O_2}(t)$ as

$$p^{c}_{O_2}(t) = \frac{RTn^{c}_{O_2}(t)}{v_c} = \frac{RT\left|\int_0^t (I^{c}_{i}(t') - I^{el}_{i}(t'))\right| dt'}{4\lambda F v_c} \quad (36)$$

It may be conveniently assumed that whenever $p^{c}_{O_2}(t)$ exceeds some critical value, cracking or delamination will occur, albeit stably [4].[6] The $p^{c}_{O_2}(t)$ is a monotonically increasing function of time. It is immediately clear that the smaller the pore volume, v_c, the lower will be the time required to pressurize to a given extent. The implication is that, once the deviation has set in ($V_C < 0$), it is quite possible that the time required for developing a sufficiently large pressure to cause delamination may be rather small—by comparison with typical expected service life of an SOFC stack. Thus, the prediction is that much of the time required for stack degradation to occur may be related to the time required for establishing abnormal behavior (for establishing conditions so that V_C becomes negative). For example, this may be due to greater oxidation of one of the interconnects (defective), or loss of contact due to seal degradation, or degradation of contact aid, resulting in an increase in resistance. Once this has occurred, subsequent cell and stack degradation by the mechanism described here may occur very fast. Indeed, experiments on oxygen separation systems have shown that degradation can occur in a matter of hours, once the commensurate conditions are established [4].

In the experiments conducted in [4], the membrane thickness was about 2 mm. It has been shown that the time required to achieve a given pressure increases with increasing membrane thickness although the dependencies are different for cation conductors and anion conductors [3,4]. In a typical electrode-supported SOFC, the electrolyte thickness is on the order of 5–30 μm instead of the 2 mm used in earlier studies [4]. The implication is that the kinetics of degradation will indeed be very fast in a typical SOFC stack, once deviation has set in. That is, virtually all of the 'incubation' time is spent in generating 'bad' conditions (cell voltage going negative). Once this happens ($V_C < 0$), the subsequent degradation may occur very fast—perhaps in a matter of minutes.

4. Possible implications concerning planar and tubular SOFC stacks

The analysis presented here suggests possible differences in propensity for stack degradation in planar and tubular stacks. In planar stacks, repeat units are series-connected with rigid separators, and often with rigid seals. Any possible variations in stack dimensions (e.g. due to differential heating or cooling, changes in seals, changes in contact aids, etc.) occurring over time, however minute, will likely generate stresses in turn causing initial weakening of interfaces, such as the interconnect/cell interface. Such events may lead to a rise in resistance—a precursor to cell and stack failure by the mechanism described here. Indeed, it is often observed that contact aids introduced to ensure a good contact between cell and interconnect or wire mesh, often bond too strongly to one of the two electrodes (e.g. cathode) or the wire mesh. Repeated heating/cooling, or even operation under fixed conditions, may lead to debonding (delamination) of such interfaces and rise in resistance, build up of pressure by the mechanism described here causing cathode delamination and subsequent degradation. In tubular stacks, on the other hand, series connections between cells are pliable/flexible and usually large stresses are not expected to develop across connections due to differential heating/cooling. Thus, the likelihood of rise in resistance and subsequent delamination as described here, is expected to be lower. The preliminary analysis thus suggests that tubular stacks may likely be more resistant to long term degradation compared to planar stacks, *assuming* there is no degradation of contacts in tubular stacks. Perhaps the reported long term durability or robustness of Siemens-Westinghouse stacks may well be related to this aspect. Insofar as planar stacks are concerned, those using flexible or compliant seals with a constant externally applied load on the stack (such as through springs located in the cold zone outside the stack) may be more resistant to degradation than stacks using rigid glass or glass ceramic seals wherein some loss of contact may occur over time due to slight dimensional changes resulting in the type of degradation described here.

5. Implications of the analysis and materials' properties

Using Eqs. (5)–(15), a number of scenarios can be envisioned based on transport properties of the membrane and interfaces, with a particular emphasis on the *electronic* transport properties. That is, even though the electronic transport is much lower than ionic transport (electrolyte being a predominantly ionic conductor), whether or not a cell will degrade under given operating conditions will mainly be dictated by the low level electronic conduction. As an example, if $r^{c}_{e} \gg r^{el}_{e}, r^{a}_{e}$ so that $r^{c}_{e}/R_e \approx 1$, then even a small magnitude of V_C (with $V_C < 0$) may lead to large pressures just inside the electrolyte under the cathode/electrolyte interface, leading to cracking and/or cathode delamination. It has been demonstrated that modest levels of applied voltage in an oxygen pumping mode can degrade YSZ, where degradation manifests as small pits in the electrolyte and delamination of electrodes [4]. In the present case, the existence of a negative voltage across a 'bad' cell in a stack leads to an analogous situation. If, on the other hand, $r^{a}_{e} \gg r^{el}_{e}, r^{c}_{e}$, so that $r^{a}_{e}/R_e \approx 1$, then the mechanism of degradation will involve electrolyte decomposition at the anode/electrolyte interface. This will require that the magnitude of $|V_C| > 1.3$ V, with $V_C < 0$. This condition is somewhat more difficult to meet, with the expectation that electrolyte degradation by decomposition (and thus cell and stack degradation), is less likely. This suggests that a somewhat larger *electronic* charge transfer resistance at the

[6] This statement ignores the fact that the pressure required to cause delamination is actually a function of the pore size (and shape), and fracture mechanical models can be used to describe the relevant equations. Here, for the purposes of a qualitative discussion, we have ignored this aspect. Ref. [4] discusses one specific case which addresses fracture mechanical considerations.

anode may be acceptable, but not at the cathode. However, as stated previously, in a stack with a large number of cells, this is also a likely scenario, and electrolyte decomposition at the anode/electrolyte interface is quite possible. Thus, depending upon interface transport properties, both mechanisms of initial deviation are likely. Unfortunately, in a typical planar stack, when voltages on individual cells are not monitored, it would be virtually impossible to observe any warning signs by simply monitoring stack voltage and stack current. That is, for all practical purposes, such occurrences leading to degradation would appear to be rather sudden, even though the development of undesirable conditions leading to deviation may have been in the making for a long time. Postmortem also may not reveal the cause (or causes) of degradation since considerable damage often occurs to cells/stack, and the initial precursor damage may leave little identifiable signature. If however the stack operation is voluntarily interrupted to examine the stack prior to the occurrence of substantial damage, if the above mechanism is operative, the identifiable signature would be the observation of cathode delamination on those cells exhibiting higher resistance than the rest of the cells. This suggests that the ability to measure voltage across each cell, especially in planar stacks, could be important in preventing catastrophic failure—assuming that the knowledge of one or more cells going 'bad' would allow one to do repairs and conduct preventative maintenance. An alternate approach may involve externally shorting the 'bad' cell.

Finally, as the occurrence of deviation is dependent on the electronic transport parameters, the present work suggests that cell and stack degradation may be prevented or suppressed or postponed by tailoring the transport properties of the membrane and the interfaces, with a particular emphasis on the low level electronic conduction. It would appear that suitable dopants could be identified towards this end.

6. Summary

A model for cell/stack degradation, based on transport properties of the membrane and electrolyte/electrode interfaces, is presented. Electronic transport, however small, is shown to be central to the development of conditions leading to cell and stack degradation. It is shown that a cell with a higher resistance compared to the rest of the cells in a stack and operating under a negative voltage will be prone to degradation, where degradation manifests as a large increase or decrease in the oxygen chemical potential in the *membrane*, $\mu_{O_2}^{membrane}$ (and thus large increase or decrease in the *membrane* p_{O_2}), just under the electrode/electrolytes interfaces.[7] Either situation may lead to stack degradation. It is also suggested that planar stacks may be more prone to such degradation than tubular stacks. If contacts degrade, however, tubular cell stacks, especially those with long axial current collection paths, may exhibit the same type of degradation as described here.

Acknowledgement

This work was funded by the U.S. Department of Energy under Grant Number DE-FG02-06ER46086.

References

[1] D. Kondepudi, I. Prigogine, Modern Thermodynamics: From Heat Engines to Dissipative Structures, John Wiley, New York, 1998.
[2] L. Heyne, Mass Transport in Oxides, vol. 296, NBS Special Publication, 1968, pp. 149–164.
[3] A.V. Virkar, J. Mater. Sci. 20 (1985) 552.
[4] A.V. Virkar, J. Nachlas, A.V. Joshi, J. Diamond, J. Am. Ceram. Soc. 73 (11) (1990) 3382.
[5] A.V. Virkar, J. Electrochem. Soc. 138 (5) (1991) 1481.
[6] A.V. Virkar, J. Power Sources 147 (2005) 8.
[7] A.V. Virkar, J. Power Sources 154 (2006) 324.
[8] F. Liu, M.G. Lagally, Phys. Rev. Lett. 76 (17) (1996) 3156–3159.
[9] C. Wagner, Proceedings of the 7th Meeting Int. Comm. on Electrochemistry Thermodynamics and Kinetics, Lindau, Butterworth, 1957, pp. 361–377.
[10] T. Kenjo, S. Osawa, K. Fujikawa, J. Electrochem. Soc. 138 (1991) 349.
[11] C.W. Tanner, K.-Z. Fung, A.V. Virkar, J. Electrochem. Soc. 144 (1) (1997) 21.
[12] J.R. Macdonald, Impedance Spectroscopy, A Wiley–Interscience Publication, New York, 1987.
[13] H.-T. Lim, A.V. Virkar, Unpublished work, 2007.
[14] D.L. Powers, Boundary Value Problems, Academic Press, New York, 1972.
[15] I. Barin, Thermochemical Data of Pure Substances: Parts I and II, VCH Publication, Weiheim, Germany, 1993.

[7] Or could also occur somewhere *within* the membrane, depending upon the relative transport parameters, as discussed in Refs. [3,4] and demonstrated experimentally in Ref. [4].